Available online at www.sciencedirect.com

SciVerse ScienceDirect

Ceramics International 39 (2013) 3585–3589

CERAMICS INTERNATIONAL

www.elsevier.com/locate/ceramint

Sol–gel synthesis and infrared radiation property of Li-substituted cordierite

Dong Zou*, Xuesong Chu, Feng Wu

Hangzhou Institute of Municipal Construction, Hangzhou 310003, China

Received 27 August 2012; received in revised form 10 October 2012; accepted 10 October 2012
Available online 17 October 2012

Abstract

The $Mg_{2-x}Al_{4+1/2x}Li_{1/2x}Si_5O_{18}$ ($0.1 \le x \le 1$) ceramics with the substitution of $(Li_{1/2}Al_{1/2})^{2+}$ for Mg^{2+} were synthesized by the sol–gel method. The characterization of the modified cordierite included X-ray diffraction, SEM, EDS and infrared radiation. The crystal structure of $Mg_2Al_4Si_5O_{18}$ with the substitution of $(Li_{1/2}Al_{1/2})^{2+}$ for Mg^{2+} changed and the amount of secondary phase increased with increasing the x value from 0.1 to 1. High infrared emissivity over 0.9 in the band of 8–14 μm at room temperature was obtained in $Mg_{2-x}Al_{4+1/2x}Li_{1/2x}Si_5O_{18}$ ($x=0.1$). The material based on cordierite with $x=0.1$ sintered at 1200 °C maintained a single phase, compact microstructure and good infrared emissivity with potential use in infrared heating.

Keywords: D. Cordierite; Sol–gel; Substitution; Infrared radiance

1. Introduction

Recently, infrared heating and drying technology has acquired considerable industrial applications by considerations of energy conservation and less pollution [1,2]. This brings a boom in research and development of high infrared emissivity materials [3–6]. In this context, the $MgO–Al_2O_3–SiO_2$ system with the main phase of cordierite with good infrared radiation has extensively attracted research interest in the past few years [7–11]. Many previously published investigations have reported on the preparation of cordierite by solid state reactions, crystallizing the glasses, the sol–gel technique, and so on [12–16]. Further, Wang et al. focused on improving the infrared emissivity of cordierite based materials [17–20]. However, to our knowledge, the cordierite based materials with high infrared emissivity are still few. According to the harmonic oscillator theory, the heterogeneous ion solution has a significant influence on the infrared radiation property of polycrystalline materials. In order to develop a high infrared emissivity material based on cordierite, in the present work, the sol–gel technique was selected to prepare the cordierite based materials and studied the effects of the substitution of $(Li_{1/2}Al_{1/2})^{2+}$ for Mg^{2+} on the crystallization behavior and infrared radiation property of $Mg_{2-x}Al_{4+1/2x}Li_{1/2x}Si_5O_{18}$ ($0.1 \le x \le 1$).

2. Experimental procedure

$Mg_{2-x}Al_{4+1/2x}Li_{1/2x}Si_5O_{18}$ ($0.1 \le x \le 1$) was prepared by sol–gel route using $Mg(NO_3)_2 \cdot 6H_2O$, $Al(NO_3)_3 \cdot 9H_2O$, Li_2CO_3 and $Si(OC_2H_5)_4$ (TEOS). The preparation process was shown in Fig. 1.

$Mg(NO_3)_2 \cdot 6H_2O$, $Al(NO_3)_3 \cdot 9H_2O$ and Li_2CO_3 dissolved in ethanol respectively. TEOS was mixed with ethanol and water by volume ratio of 1:2:2 and stirred at room temperature for 0.5 h. Subsequently, $Mg(NO_3)_2 \cdot 6H_2O$, $Al(NO_3)_3 \cdot 9H_2O$ and Li_2CO_3 solutions were put into partially hydrolyzed TEOS and stirred for 1 h to obtain a clear solution. The pH value of mixed solution was turned to 10 in the experimental process by ammonia. Then the mixture was stirred at 60 °C for 6 h to get a semitransparent gel. Consequently, the obtained gel was dried at 100 °C for 24 h and the dried gel was thermally treated at 1000–1200 °C for 2 h in furnace.

*Corresponding author. Tel./fax: +86 5718 7018725.
E-mail address: zoudong@zju.edu.cn (D. Zou).

0272-8842/$ - see front matter © 2012 Elsevier Ltd and Techna Group S.r.l. All rights reserved.
http://dx.doi.org/10.1016/j.ceramint.2012.10.185

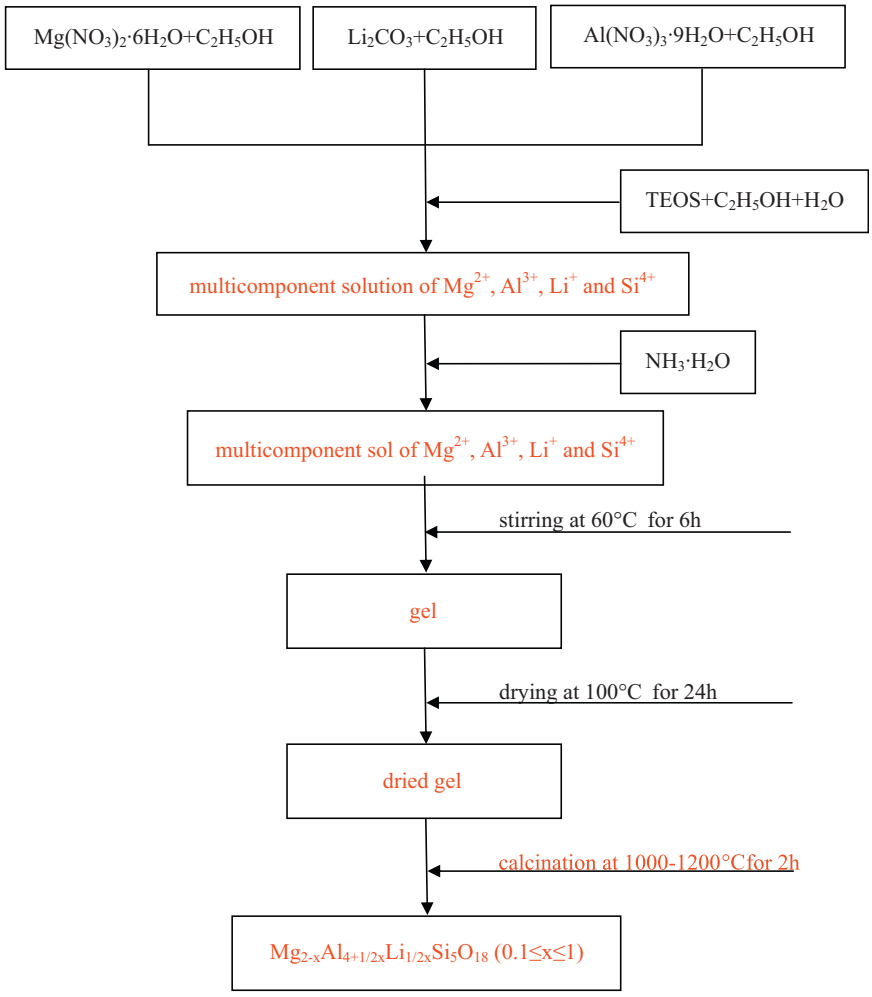

Fig. 1. Flow chart of the sol–gel preparation of $Mg_{2-x}Al_{4+1/2x}Li_{1/2x}Si_5O_{18}$ ($0.1 \le x \le 1$).

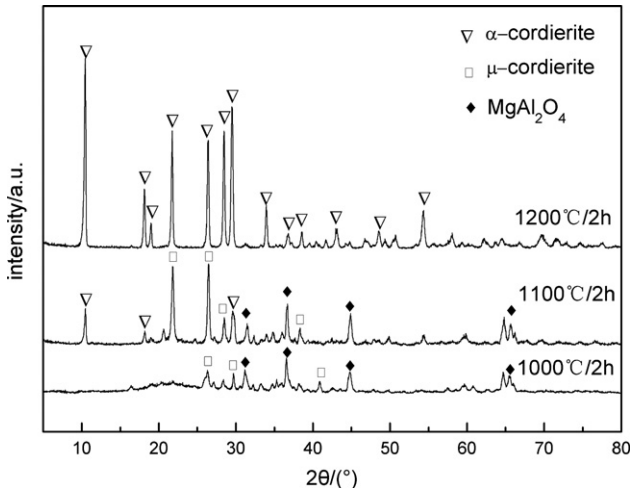

Fig. 2. XRD patterns of $Mg_{2-x}Al_{4+1/2x}Li_{1/2x}Si_5O_{18}$ ($x=0.1$) powder sintered at different temperatures for 2 h.

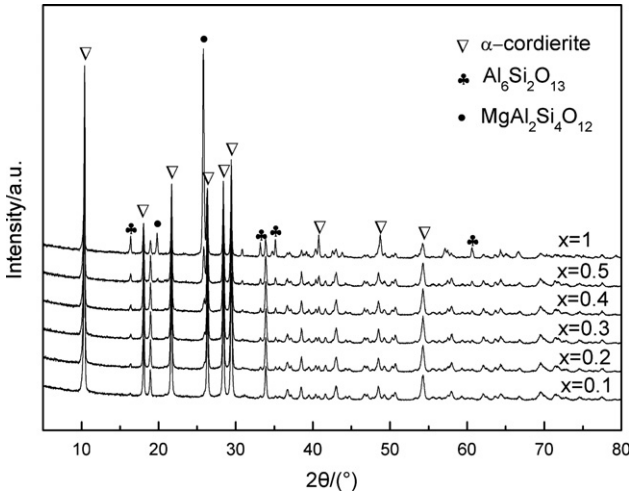

Fig. 3. XRD patterns of $Mg_{2-x}Al_{4+1/2x}Li_{1/2x}Si_5O_{18}$ ($0.1 \le x \le 1$) powder sintered at 1200 °C for 2 h.

The crystalline phases of the sintered samples were examined by X-ray powder diffraction using CuK_α radiation (XRD Rigaku, D/max-RA). The microstructures of specimens were observed by scanning electron microscopy (SEM, FEI SIRION-100) and the compositions were analyzed by energy-dispersive spectroscopy (EDS, EDAX

GENENIS-4000). The infrared radiation characteristics were examined using an infrared radiation tester (IRE-2, Shanghai Institute of Technical Physics, CAS, China). The size of each sample was Φ 80 mm × 3 mm. Measurements were carried out at room temperature.

3. Results and discussion

The X-ray diffraction patterns of $Mg_{2-x}Al_{4+1/2x}Li_{1/2x}Si_5O_{18}$ ($x=0.1$) powder sintered at 1000 °C, 1100 °C and 1200 °C for 2 h each are given in Fig. 2. It can be seen that the crystal structures of samples change with increasing temperature. At low temperature (1000 °C), the main phase is $MgAl_2O_4$ (JCPDS no. 21-1152) with a small quantity of μ-cordierite (JCPDS no. 14-0249) and amorphous phase. With further heating at 1100 °C, α-cordierite (JCPDS no. 13-0293) appears together with μ-cordierite and $MgAl_2O_4$. At 1200 °C, a single α-cordierite phase is found which indicates α-cordierite generates through the intermediate phases of μ-cordierite and $MgAl_2O_4$. These results are comparable with the previous report [21].

Fig. 3 shows the XRD patterns of $Mg_{2-x}Al_{4+1/2x}Li_{1/2x}Si_5O_{18}$ ($0.1 \le x \le 1$) powder sintered at 1200 °C for 2 h. It can be observed that the main phase of samples is α-cordierite with a small amount of $Al_6Si_2O_{13}$ (JCPDS no. 15-0776) and $MgAl_2Si_4O_{12}$ (JCPDS no. 27-0716) which only appears when $x=1$. This indicates that modified cordierite with $x=0.1$ could form solid solution. However,

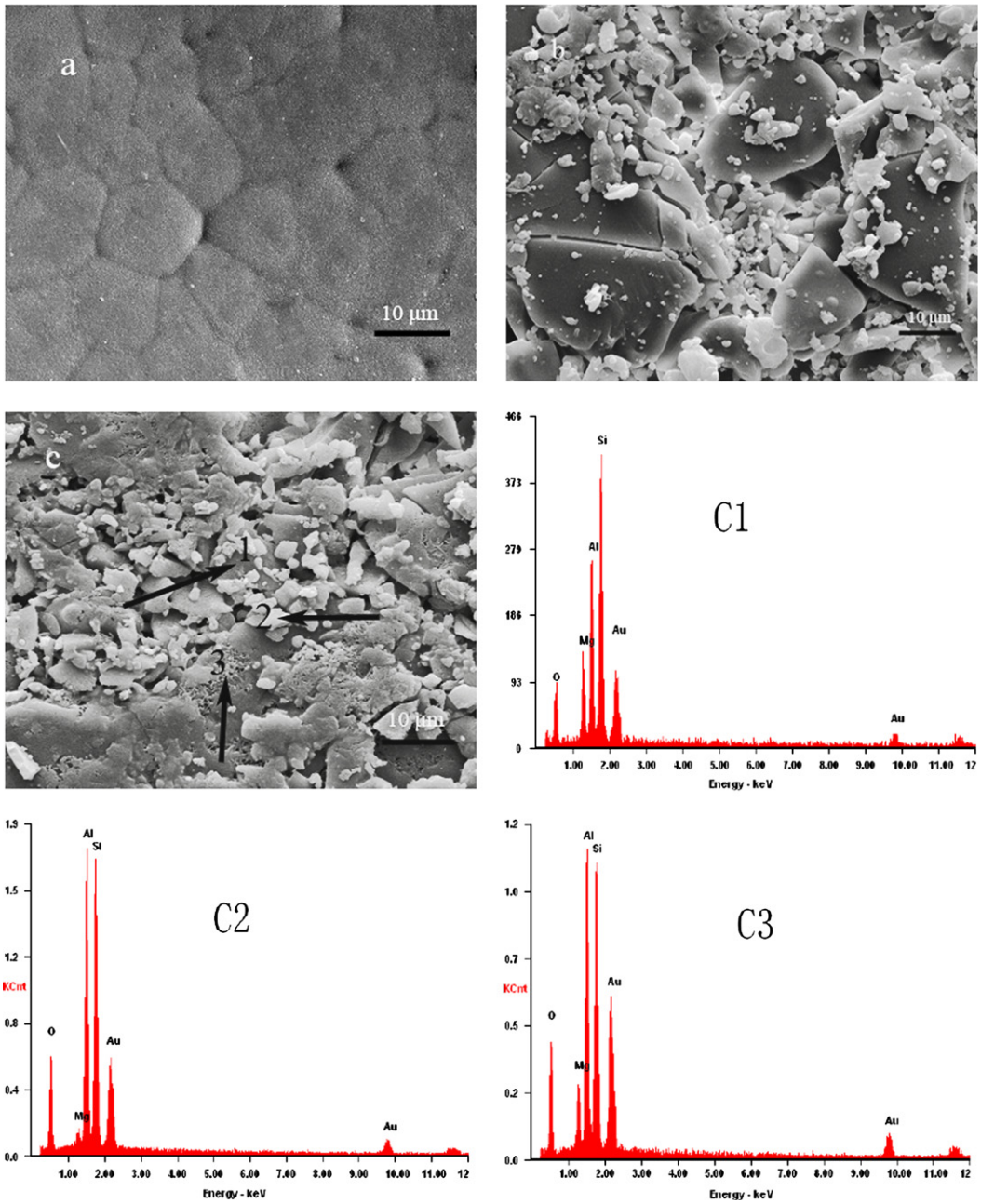

Fig. 4. SEM micrographs of $Mg_{2-x}Al_{4+1/2x}Li_{1/2x}Si_5O_{18}$ (a) $x=0.1$, (b) $x=0.3$, and (c) $x=1$ and energy spectrum analysis of corresponding spots in (c).

Table 1
Infrared radiance of $Mg_{2-x}Al_{4+1/2x}Li_{1/2x}Si_5O_{18}$ ($0.1 \le x \le 1$) and pure cordierite (at room temperature).

X	0	0.1	0.2	0.3	0.4	0.5	1.0
F1	0.82	0.91	0.87	0.87	0.86	0.85	0.80
F2	0.85	0.93	0.91	0.90	0.90	0.88	0.83

F1—the radiance at 1–22 μm waveband; F2—the radiance at 8–14 μm waveband.

the secondary phase $Al_6Si_2O_{13}$ appears with increasing x value, and the quantity of $Al_6Si_2O_{13}$ also increases with increasing the substitution of $(Li_{1/2}Al_{1/2})^{2+}$ for Mg^{2+}.

The SEM micrographs of $Mg_{2-x}Al_{4+1/2x}Li_{1/2x}Si_5O_{18}$ ($x=0.1$, $x=0.3$, $x=1$) sintered at 1200 °C for 2 h are shown in Fig. 4. $Mg_{2-x}Al_{4+1/2x}Li_{1/2x}Si_5O_{18}$ ($x=0.1$) shows a dense microstructure and approximately rounded grains. However, with increasing the amount of the substitution of $(Li_{1/2}Al_{1/2})^{2+}$ for Mg^{2+}, it is clear that the morphologies of grains turn irregular and porosity appears which attribute to the evaporation of Li at high temperature [22,23]. Fig. 4(c1), (c2) and (c3) shows the composition of the grains in Fig. 4(c) nearly corresponding to $Mg_2Al_4Si_5O_{18}$, $Al_6Si_2O_{13}$, and $MgAl_2Si_4O_{12}$, respectively. The results confirm the secondary phase observed in the XRD analysis.

The measurement results of infrared radiance of $Mg_{2-x}Al_{4+1/2x}Li_{1/2x}Si_5O_{18}$ ($0.1 \le x \le 1$) and pure cordierite for comparison are shown in Table 1. It is obvious that the infrared radiance of the $Mg_{2-x}Al_{4+1/2x}Li_{1/2x}Si_5O_{18}$ ($0.1 \le x \le 1$) is much higher than that of the commercial pure cordierite except when $x=1$ which may be due to the formation of $MgAl_2Si_4O_{12}$ with lower infrared radiance. It can be seen from Table 1 that the infrared radiance of $Mg_{2-x}Al_{4+1/2x}Li_{1/2x}Si_5O_{18}$ ($x=0.1$) is highest which means that the formation of cordierite solid solution greatly enhances the infrared radiance of substituted cordierite. However, the infrared radiance decreases with increasing the secondary phase $Al_6Si_2O_{13}$, but is still higher than pure cordierite. Thus, it indicates that the raising of infrared radiance is attributed to the formation of solid solution which changes the crystal structure. Because the radii of $(Li_{1/2}Al_{1/2})^{2+}$ and Mg^{2+} are different and the amount of Al^{3+} changed, the order degree of Al/Si in crystal structure of cordierite decreases which causes a distortion of the crystal lattice. This enhances the effects of anharmonic vibration of the polar lattice, the coupled action of phonon, and phonon combination radiation. As a result, the infrared radiance of this material improves.

4. Conclusions

In this study, cordierite based material was prepared by the sol–gel method and the effects of substitution of $(Li_{1/2}Al_{1/2})^{2+}$ for Mg^{2+} on crystallization behavior and infrared radiant property of $Mg_{2-x}Al_{4+1/2x}Li_{1/2x}Si_5O_{18}$ ($0.1 \le x \le 1$) have been investigated. Appropriate substitution can form solid solution, but secondary phase appeared with increasing the substitution of $(Li_{1/2}Al_{1/2})^{2+}$ for Mg^{2+}. The appropriate substitution of $(Li_{1/2}Al_{1/2})^{2+}$ for Mg^{2+} in cordierite crystal structure could effectively improve the infrared emissivity (over 0.9), which made it a promising candidate in infrared heating.

References

[1] S. Jons, S. Alonso, F. Taracena-Sanz, Infrared drying: a leather finishing application, Journal of the American Leather Chemists Association 101 (2006) 105–111.
[2] N.K. Rastogi, Recent trends and developments in infrared heating in food processing, Critical Reviews in Food Science and Nutrition 52 (2012) 737–760.
[3] W. Chen, W.P. Ye, X.D. Cheng, W. Duan, F. Mao, D.L. Li, Preparation, microstructure and properties of $NiO–Cr_2O_3–TiO_2$ infrared radiation coating, Journal of Materials Science and Technology 25 (2009) 695–698.
[4] Y. Zhang, J. Lin, D.J. Wen, Structure, infrared radiation properties and mossbauer spectroscopic investigations of $Co_{0.6}Zn_{0.4}Ni_xFe_{2-x}O_4$ ceramics, Journal of Materials Science and Technology 26 (2010) 687–692.
[5] J. Manara, M. Arduini-Schuster, M. Keller, Infrared-optical characteristics of ceramics at elevated temperature, Infrared Physics and Technology 54 (2011) 395–402.
[6] C.B. Ju, Y.S. Wang, D.W. He, Q. Gao, L. Gao, M. Fu, Synthesis and infrared property of polyaniline/phase-change nanocapsule composite, Journal of Nanoscience and Nanotechnology 11 (2011) 9665–9670.
[7] M.A. Camerucci, G. Urretavizcaya, A.L. Cavalieri, Sintering of cordierite based materials, Ceramics International 29 (2003) 159–168.
[8] Z. Acimovic, L. Pavlovic, L. Trumbulovic, L. Andric, M. Stamatovic, Synthesis and characterization of the cordierite ceramics from non-standard raw materials for application in foundry, Materials Letters 57 (2003) 2651–2656.
[9] R. Goren, H. Gocmez, C. Ozgur, Synthesis of cordierite powder from talc, diatomite and alumina, Ceramics International 32 (2006) 407–409.
[10] E. Yalamac, S. Akkurt, Additive and intensive grinding effects on the synthesis of cordierite, Ceramics International 32 (2006) 825–832.
[11] J.M. Benito, X. Turrillas, G.J. Cuello, A.H. De Aza, S. De Aza, M.A. Rodriguez, Cordierite synthesis: a time-resolved neutron diffraction study, Journal of the European Ceramic Society 32 (2012) 371–379.
[12] S. Tamborenea, A.D. Mazzoni, E.F. Aglietti, Mechanochemical activation of minerals on the cordierite synthesis, Thermochimica Acta 411 (2004) 219–224.
[13] J.R. Gonzalez-Velasco, R. Ferret, R. Lopez-Fonseca, M.A. Gutierrez-Ortiz, Influence of particle size distribution of precursor oxides on the synthesis of cordierite by solid-state reaction, Powder Technology 153 (2005) 34–42.
[14] N.J. Azin, M.A. Camerucci, A.L. Cavalieri, Crystallisation of non-stoichiometric cordierite glasses, Ceramics International 31 (2005) 189–195.
[15] A.M. Menchi, A. Scian, Mechanism of cordierite formation obtained by the sol–gel technique, Materials Letters 59 (2005) 2664–2667.
[16] R. Ianos, I. Lazau, C. Pacurariu, Solution combustion synthesis of alpha-cordierite, Journal of Alloys and Compounds 480 (2009) 702–705.
[17] S.M. Wang, K.M. Liang, High infrared radiance glass-ceramics obtained from fly ash and titanium slag, Chemosphere 69 (2007) 1798–1801.
[18] S.M. Wang, K.M. Liang, Crystallization behavior and infrared radiation property of nickel–magnesium cordierite based glass-ceramics, Journal of Non-Crystalline Solids 354 (2008) 1522–1525.

[19] S.M. Wang, F.H. Kuang, Sol–gel preparation and infrared radiation property of boron-substituted cordierite glass-ceramics, Journal of Materials Science and Technology 26 (2010) 445–448.
[20] S.M. Wang, F.H. Kuang, Q.Z. Yan, C.C. Ge, L.H. Qi, Crystallization and infrared radiation properties of iron ion doped cordierite glass-ceramics, Journal of Alloys and Compounds 509 (2011) 2819–2823.
[21] M.K. Naskar, M. Chatterjee, A novel process for the synthesis of cordierite ($Mg_2Al_4Si_5O_{18}$) powders from rice husk ash and other sources of silica and their comparative study, Journal of the European Ceramic Society 24 (2004) 3499–3508.
[22] M. Pollet, S. Marinel, Low temperature sintering of $CaZrO_3$ using lithium fluoride addition, Journal of the European Ceramic Society 23 (2003) 1925–1933.
[23] J.X. Tong, Q.L. Zhang, H. Yang, J.L. Zou, Low-temperature firing and microwave dielectric properties of $Ca[(Li_{1/3}Nb_{2/3})_{0.84}Ti_{0.16}]O_{3-\delta}$ ceramics for LTCC applications, Journal of the American Ceramic Society 90 (2007) 845–849.